Similar NoE Tensor Workshop, Las Palmas, November 2006

DT-MRI CONNECTIVITY AND/OR TRACTOGRAPHY ? : TWO NEW ALGORITHMS

Burak Acar
Boğaziçi University
Electrical & Electronics Eng. Dept.
BUSIM/VAVlab
İstanbul, Turkey
email : acarbu@boun.edu.tr
URL : www.vavlab.ee.boun.edu.tr

ABSTRACT

The goal of this manuscript is to give a brief review of DT-MRI analysis and pose the question of whether it is the connectivity or the tractography approach that we should focus on. We state the advantages and the disadvantages of these two approaches and review two new methods recently proposed for DT-MRI analysis, namely, the SMT (Split & Merge Tractography) and LoS (Lattice of Springs Modeling). Both methods belong to the class of algorithms that aim at overcoming the inherent limitations of conventional Fiber Tractography.

1. INTRODUCTION

It is of utmost importance to understand what the DT-MRI signal represents in order to develop adequate analysis and visualization methods. DT-MRI measures the average signal attenuation within a small subvolume (i.e. a voxel) due to water molecules spinning out-of-phase.

The basis of MRI is to *perturb* the water molecules (the dipoles) that were aligned in a constant magnetic field ($B_0 \approx 1 - 7Tesla$) and let them re-orient themselves with B_0 during which the dipoles rotate around B_0 according to the Bloch's Equation. This rotation causes a temporal change in total magnetic field which induces a time-varying current at the receiving coils of the MR scanner. The time it takes for the dipoles to fully relax depends on the environment (i.e. the tissue). Thus, the amount of current induced is proportional to the number of dipoles (i.e water concentration) and the tissue type. These current measurements are transformed to monochromatic images in which each pixel value is also a function of water concentration and tissue type [1].

In DT-MRI, extra spatially varying magnetic fields, the so called Diffusion Weighting Gradients (DWG), G, are applied together with B_0. Due to this added G field, the water molecules under continuous brownian motion experience different total magnetic field at different locations. This causes then to rotate at different frequencies, i.e. to be out-of-phase. The effect of out-of-phase dipoles on the induced current is attenuation. So, the amount of attenuation in the received signal (equivalently in the diffusion weighted MR images) is a function of the brownian motion (i.e diffusion) of water molecules and the applied G field.

This phenomenon is described by the superposition of the Bloch's Equation and the Diffusion Equation as follows :

$$\frac{\partial M}{\partial t} = \gamma M \times (B_0 + G) - \left(M - \begin{bmatrix} 0 \\ 0 \\ M_z \end{bmatrix} \right) \begin{bmatrix} \frac{1}{T_2} & 0 & 0 \\ 0 & \frac{1}{T_2} & 0 \\ 0 & 0 & \frac{1}{T_1} \end{bmatrix} - \nabla \cdot D \nabla M \qquad (1)$$

[1] In order to compute this for each voxel in 3D, spatial coding magnetic fields must be applied, which is equivalent to saying that B_0 must be a function of space. For the sake of clarity, we ignored spatially varying B_0 and assumed that our space consists of a single voxel.

where the first term is the rotation, the second term is the relaxation and the third term is the diffusion components of the temporal change of the magnetic field, consequently of the induced current which is related to the MR image. The solution to the transverse component of M, i.e. $m = M_x + jM_y$, just before the imaging sequence, is given as,

$$m(TE) = m^0 exp(-\sum_{i,j} b_{ij} D_{ij}) \ , (i,j) \in \{x,y,z\} \tag{2}$$

The six independent components of the symmetric diffusion tensor D can be computed using at least 6 linearly independent equations of the form of Equation 2. When the diffusing water molecules are in a restricted media, such as nerve fibers, then the physical barriers (the membrane) limit the space into which the particles diffuse, thus the apparent diffusion pattern is correlated with these barriers, i.e. the structure. The underlying assumption of DT-MRI tractography is that the principal diffusion direction is tangent to the fiber.

The diffusion component of Equation 1 is the well known diffusion PDE based on Fick's Law which establishes the relation between concentration gradient and flux as $F_k = -D_{kl} \frac{\partial C}{\partial x_l}$ for $(k,l) \in \{1,2,3\}$ in 3D. However, as suggested by Liu et al. in [1], if the gaussianity assumption of the underlying diffusion process is removed, then the physical process can be (should be) characterized by using higher order diffusion tensors. This corresponds to generalizing the Fick's Law as

$$F_k = -D^{(2)}_{kl} \frac{\partial C}{\partial x_l} - D^{(3)}_{klm} \frac{\partial^2 C}{\partial x_l \partial x_m} - D^{(4)}_{klmn} \frac{\partial^3 C}{\partial x_l \partial x_m \partial x_n} - \dots \tag{3}$$

The details of Generalized Diffusion Tensor can be found in [1]. The points we would like to emphasize regarding the nature of the DT-MRI data are,

- The second order diffusion tensor is a second order approximation to the diffusion process which assumes a Gaussian distribution of diffusing particles
- The measured diffusion tensor in DT-MRI is computed using the average MR signal acquired from a subvolume (a voxel)

Consequently, the DT-MRI data provides a coarse picture of the underlying fiber structure. Not only its spatial resolution is insufficient to identify the individual fibers, but also its modeling of the diffusion process relies on the gaussianity assumption. Nevertheless, DT-MRI data does provide useful clinical information as has been shown by numerous studies in literature.

There are two basic approaches in utilizing the information DT-MRI provides : Fiber Tractography and Connectivity Mapping. The former approach relies on the principal diffusion direction and attempts to reconstruct the fiber that passes through a given point. The basic tool used for tractography is numerical integration of the principal diffusion direction (the major eigenvector of the diffusion tensor) among which the most popular method is the 4th order Runge-Kutta [2]. Fiber tractography is prone to cumulative errors, can not overcome the partial volume effect and disregards part of the information embedded in the diffusion tensor (which itself is an approximation based on gaussianity assumption). The latter approach attempts to utilize the true nature of the DT-MRI data, i.e. the gaussian diffusion process, by estimating a connectivity map. They consider each and every possible connection with weights set by the dataset. Several approaches in this group are based on some sort of Monte-Carlo simulations of the random walk model [3, 4, 5]. Lenglet et al., on the other hand, recasted the connectivity problem to Riemannian differential geometry framework where they defined their local metric tensor using the DTI data and solved for geodesics [6].

Probably, the most important point that differentiates these two approaches is their behaviour at problematic regions such as *crossing* and *kissing* fibers. The tractography methods either pretends to follow a single fiber by choosing a direction to proceed or stops tracking, whereas the connectivity mapping based methods allow for branching. Although branching is not correct anatomically, presenting the DT-MRI data in this way is more loyal to the nature of the acquired data (localized gaussian maps of diffusing particles) and allows the users to interpret is. Thus, we can say that connectivity mapping is a more direct way of communicating the information embedded in DT-MRI data. However, it is not trivial to interpret connectivity maps.

One possible way to find a compromise between the two approaches is to develop innovative tensor visualization techniques and user interfaces. With such techniques, it can be possible to present the information in DT-MRI data directly and effectively to the users, who can use their own expertise to draw conclusions. There are several groups in SIMILAR NoE (www.similar.cc) working on tensor visualization and user interface tools. A selection of manuscripts based on such research is included in this proceedings as well. Our focus, however, will be two methods recently proposed for DT-MRI analysis by VAVlab (Boğaziçi University, Turkey) : The Lattice-Of-Springs (LoS) method and The Split & Merge Tractography (SMT).

2. LOS : THE LATTICE OF SPRINGS MODEL

The Lattice-of-Springs model is based on forming a 3D regular lattice composed of springs whose spring constants are proportional to local connectivity[2]. This lattice is used to efficiently compute connectivity maps for a given set of seed points.

In general, connectivity can be interpreted as a measure which is proportional to the qualitative similarity and spatial proximity of the units contained in data to be analyzed. In the case of DT images, where we are trying to reveal a functional connectivity, qualitative assessment of tensors becomes crucial in order to construct an appropriate model. We have to consider some certain features embedded in a DT image as indicators of connectivity. In general, the connectivity measure between two tensors can be visualized in terms of the volume overlap of their ellipsoids centered at the corresponding voxel coordinates. This interpretation will take the relative features of tensors into consideration such as their respective locations, sizes, orientations and shapes. A similar but simpler metric, that we proposed and used in this study is the so-called distance scaled mutual diffusion coefficient K. Given two tensors $\mathbf{D}_1$ and $\mathbf{D}_2$, located at $\mathbf{r}_1$ and $\mathbf{r}_2$, respectively, we define their connectivity K_{12} as :

$$K_{12} = \frac{[(\mathbf{v}^T\mathbf{D}_1\mathbf{v})(\mathbf{v}^T\mathbf{D}_2\mathbf{v})]^\gamma}{\delta^2} \tag{4}$$

where $\mathbf{v} = (\mathbf{r}_1 - \mathbf{r}_2)/\delta$ and $\delta = \|\mathbf{r}_1 - \mathbf{r}_2\|_2$. Thus, K reflects the mutual influence of tensor pairs by giving the distance scaled product of their diffusion coefficients evaluated in the unit direction of their Euclidean link and raised to the power γ, which will be used as a tuning parameter. For the time being we take γ to be 1. We can construct a physical system, based on K_{ij}'s which reflect the connectivity pattern within DTI data.

Let $\Omega = [0, a] \times [0, b] \times [0, c] \subseteq \Re^3$ be our image domain, and let $\mathbf{D} : \Omega \rightarrow \Re^3 \times \Re^3$ be the given tensor field. We propose that the sought connectivity map $u : \Omega \rightarrow \Re$ with respect to a given seed point $(x_0, y_0, z_0) \in \Omega$ is the stationary pattern of a physical spring system defined as follows : Each voxel of the domain corresponds to a node and potential at seed node $u(x_0, y_0, z_0)$ is set to 1, which is kept constant in time. For each pair of adjacent nodes, a spring is associated with a stiffness, that is set to the mutual diffusion coefficient (Eqn. 1) evaluated for the adjacency of that particular pair. Thus, if we consider 6-neighborhood (N_6) on a regular 3D grid with δ-spacing in all directions, this model will correspond to 6 "neighbor springs" acting on each node and a node at $\mathbf{r}_i = (x, y, z)^T$ would share the following spring constant with respect to its immediate neighbor $\mathbf{r}_j = (x - \delta, y, z)^T$:

$$K_1(x, y, z) = \frac{(\mathbf{e}_1^T\mathbf{D}(x, y, z)\mathbf{e}_1)(\mathbf{e}_1^T\mathbf{D}(x - \delta, y, z)\mathbf{e}_1)}{\delta^2} \tag{5}$$

where $\mathbf{e}_1 = (1, 0, 0)^T//(\mathbf{r}_i - \mathbf{r}_j)$ is the unit vector of the orthonormal basis. Remaining constants of neighbor springs $K_2, ..., K_6$ are defined similarly with $\mathbf{e}_2 = (0, 1, 0)^T$ and $\mathbf{e}_3 = (0, 0, 1)^T$. We set spring elongations as the local directional differences of u (for instance as $u(x, y, z) - u(x - \delta, y, z)$ for K_1), such that they force u to be equal to the corresponding immediate neighbor. Finally, an extra

[2]This section is taken from our manuscript published in MICCAI2005 proceedings [7]. The development of an improved version of the LoS algorithm is currently in progress and is expected to be submitted for publication soon.

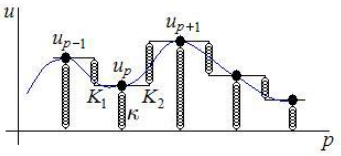

Fig. 1. Illustration of proposed spring system for a 1D curve (solid line), dots represent the nodes, spring constants are given for the specific node u_p.[7]

spring, the so-called "ground spring" with a constant stiffness κ, is also attached to all nodes, with the elongation being u and forcing u to be 0. This is necessary to justify our model for revealing connectivity, which will be explained next. The resulting spring system can be visualized in Figure 1 for a 1D curve. With this model, total potential energy stored will be given as :

$$V_{springs} = \frac{1}{2}\kappa u^2 + \sum_{n=1}^{6} V_n \tag{6}$$

where $V_1 = \frac{1}{2}K_1[u(x,y,z) - u(x-\delta,y,z)]^2$ and $V_2, ...V_6$ are defined similarly. In order to associate this potential energy to the point (x,y,z) rather than to the springs, the latter six energy terms due to the neighbor connections should further be halved, as if they are equally shared with the corresponding neighbor. We let $\delta \rightarrow 0$ assuming that we have infinite resolution, such that V can be approximated to a continuous function, enabling us to interpret the system better. Inserting K_n's common denominator δ^2 and taking the limit, we obtain :

$$V(u,u_x,u_y,u_z) = \frac{1}{2}(\kappa u^2 + d_{11}^2 u_x^2 + d_{22}^2 u_y^2 + d_{33}^2 u_z^2) \tag{7}$$

where d_{jj} $(j = 1,2,3)$ are the diagonal elements of $\mathbf{D}$ as can easily be derived from Equation 5. We can put the current problem into a variational one, where the connectivity map u with respect to the seed at (x_0,y_0,z_0) can be found by minimizing the following energy functional :

$$J(u) = \int_\Omega V(u,u_x,u_y,u_z)d\Omega \tag{8}$$

assuming Neumann boundary conditions on $\partial\Omega$, and an extra seed condition $u(x_0,y_0,z_0) = 1$. Corresponding Euler-Lagrange equation is :

$$\kappa u - \frac{d}{dx}(d_{11}^2 u_x) - \frac{d}{dy}(d_{22}^2 u_y) - \frac{d}{dz}(d_{33}^2 u_z) = 0 \tag{9}$$

It is easy to show that fixing $u(x_0,y_0,z_0)$ to 1 for an interior point of Ω, does not change the Euler-Lagrange equation since $J(u)$ can be rewritten as a sum of several integrals evaluated at Cartesian subregions, each having (x_0,y_0,z_0) at their boundaries and sharing the same integrand. The physical interpretation of our model is as follows : A connected spring system, which is only lifted at (x_0,y_0,z_0) to a constant level of 1 and kept there, achieves its stationary pattern by minimizing its total potential energy. Nodes other than the seed try to come to zero due to the ground springs, but they will be lifted up as well, in proportion to their connectivity to the stationary seed node. Hence, the stationary pattern will be equivalent to the sought connectivity map with respect to the seed node.

Temporally evolving a given initial u_0 at a rate determined by the negative of the left term of Equation 9, by a steepest descent scheme, we obtain the following PDE :

$$u_t = -\kappa u + \frac{d}{dx}(d_{11}^2 u_x) + \frac{d}{dy}(d_{22}^2 u_y) + \frac{d}{dz}(d_{33}^2 u_z) = -\kappa u + \nabla \bullet (\widetilde{\mathbf{D}}\nabla u) \tag{10}$$

where $\widetilde{\mathbf{D}}$ is a diagonal matrix with squared diagonal entries of $\mathbf{D}$. The same equation could be obtained with another $\widetilde{\mathbf{D}}$, using different neighborhood (and/or spring) definitions. In any case, resulting PDE can be considered as a modified diffusion process, with a seed condition $u(x_0, y_0, z_0) = 1$ and an extra term $-\kappa u$, keeping u attached to the ground. Thus, as $t \rightarrow \infty$, u does not get totally flat. If we interpret the model in 2D, a structure sensitive tent-like pattern will be obtained with its maximum at the seed.

Numerical implementation of such a map evolution scheme can easily be accomplished by anisotropic diffusion filters with the specified modifications and an initial map :

$$u_0(x, y, z) = \begin{cases} 1 & \textit{if } (x, y, z) = (x_0, y_0, z_0) \\ 0 & \textit{otherwise} \end{cases} \tag{11}$$

Keeping the model in its discrete form from the beginning, we can get the discrete version of Equation 8 as :

$$J(u) = \sum_p \{\kappa u_p^2 + \frac{1}{2} \sum_{n=1}^{N} K_{pn}(u_p - u_{pn})^2\} \tag{12}$$

where p is the voxel index and N is the number of neighbors. u_{pn} and K_{pn} stand for the n^{th} neighbor of the p^{th} node and its associated spring constant, respectively. $\frac{1}{2}$ scales the potential energy of neighbor springs, since they are counted twice in the outer summation. Now, writing the discrete Euler-Lagrange equation of this functional, we obtain :

$$\kappa u_p + \sum_{n}^{N} K_{pn}(u_p - u_{pn}) = 0 \tag{13}$$

This equation says that along an extremal, the total spring force applied to each node is zero. This could also be observed by rewriting Equation 9 in a discrete form where space derivatives are replaced with central differences.

Seeking for the connectivity as a PDE evolution with diffusion filters, will bring the common trade-off between stability and rate of convergence.We propose, another map evolution technique, which mimics the diffusion process in the light of the balanced force condition imposed by discrete Euler-Lagrange equation. The idea is, not to calculate the update u_t, but iteratively solve for a new u_p, which makes u_t vanish at p. "Balance in the neighborhood" condition dictated by Equation 13, locally and explicitly gives :

$$u_p = \frac{\sum_n^N K_{pn} u_{pn}}{\kappa + \sum_n^N K_{pn}} \tag{14}$$

This scheme with $\kappa = 0$ would be the same as assigning a weighted neighborhood average to each u_p, but with a spatially varying kernel coming from the local image structure. In fact, this adaptive directional smoothing constitutes the essence of the diffusion filtering, hence it can be interpreted to be equivalent to the diffusion process [5]. Equation 14 has a similar computational cost to Equation 10, but a higher convergence rate. Moreover, stability is naturally provided by the bounds specified by local neighborhood of u_{pn}'s.

Figure 2, reprinted from [7] with the addition of tracts computed based on the connectivity map, depicts four connectivity maps computed for a single seed point selected on the corpus callosum. Each map corresponds to a different γ value, ranging from 1 to 10. Note that, as γ increases, the influence of the principal diffusion direction over the others is enhanced, thus we get connectivity map the follows the true anatomy much better. The computed tracts are computed by numerical integration along the direction orthogonal to the gradient of the connectivity map, in other words, they follow the ridges of the map. We would like to refer the reader to VAVlab web page for the most recent results and publications.

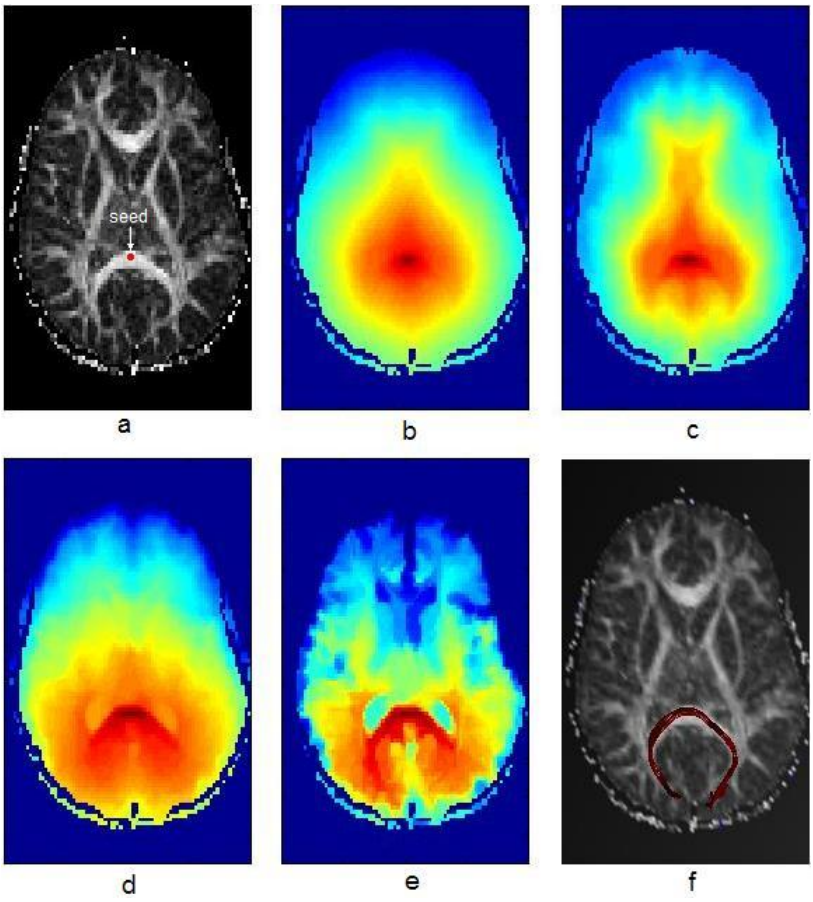

Fig. 2. Connectivity maps are computed for a single seed point on the corpus callosum for different values of γ. a) The FA map with the seed point ; Connectivity maps with b) $\gamma = 1$, b) $\gamma = 2$, b) $\gamma = 4$, b) $\gamma = 10$; e) The tracts computed by following the direction orthogonal to the gradient of the connectivity map, starting from the seed point.

3. SMT : SPLIT & MERGE TRACTOGRAPHY

Split & Merge Tractography (SMT)[8, 9] proposes a new method for fiber tractography that attempts to unify the advantages of the two aforementioned approaches, the fiber tractography and the connectivity analysis. It is a Markov Chain Monte Carlo (MCMC) technique that uses sequential sampling from an unknown distribution of samples, which are fiber tracts in this case. However, unlike previously proposed methods that exploit similar ideas for DT-MRI fiber tractography, the samples are not the full tracts but rather clusters of short tracts. The underlying rationale behind this is to avoid the error accumulation present in conventional fiber tracking. Each infinitesimal step in conventional fiber tracking (i.e. the methods based on numerical integration of the principal diffusion direction) increases the overall error. SMT, on the other hand, avoids such error accumulation by using short tracts, all computed using 4th order Runge-Kutta fiber tractography. This is the *splitting* step. The *merging* step is composed of estimating a co-occurrence matrix, M, for this abundant set of short tracts. A single element of M, namely M_{ij}, represents the probability of having the short tract S_i and S_j on the same fiber/cluster. The sequential sampling strategies gets into play at this stage of SMT. As explained below, we propose to use a direct approach of estimating M and a Metropolis-Hastings Algorithm based approach [10]. The user interface of SMT asks for *seed tracts*, which is the set of short tracts the pass through the user selected region of interest. SMT displays all the short tracts that are in the same cluster with any one of the seed tracts with a probability higher than a user selected threshold, which itself can be varied.

Let Γ_i be a true cluster of short tracts, i.e. a set of short tracts that are on the same fiber. Let S_i be a member of this cluster, typically S_i is the user selected seed string. Then, SMT aims at estimating

$$M_{ji} = P(S_j \in \Gamma_i | S_i \in \Gamma_i) \; , M_{ij} = M_{ji} \; , i, j = 1, \cdots, N \tag{15}$$

where N is the total number of short tracts that populates the complete brain. This estimation can be done using *a)* Direct Forward/Backward Tracking Strategy, *b)* Sequential Sampling Strategy.

The Direct Tracking approach is the simplest and the most trivial way to attack the problem. It is very similar to numerical integration based tractography. Let $S_i^{(k)}; i = 1, \cdots, N; k = 1, 2$ represent the k^{th} endpoint of S_i, without any specific ordering of endpoints. For a given seed tract S_i, the Direct Tracking starts by building a bridge/link between $S_i^{(1)}$ and the $S_j^{(k)}$ with the highest probability of being connected to $S_i^{(1)}$. If we denote the position of $S_i^{(k)}$ with $r_i^{(k)}$ and the diffusion tensor at that position with $D_i^{(k)}$, then that probability can be assumed to be given by

$$c_{i \rightarrow j} = P(r_i^{(1)}, r_j^{(k)}) = (\frac{1}{4\pi\tilde{D}})^{\frac{3}{2}} exp\left(\frac{-\|r_i^{(1)} - r_j^{(k)}\|^2}{4\pi\tilde{D}}\right) \; , \tilde{D} = (r_i^{(1)} - r_j^{(k)})^T D_i^{(1)} (r_i^{(1)} - r_j^{(k)}) \tag{16}$$

This is nothing but the Gaussian distribution as represented by $D_i^{(1)}$. Without loss of generality, let the selected end-point be $k = 2$ at all times. Having determined j, we increment M_{ij} and M_{ji} by one and repeat the whole process starting from $r_j^{(1)}$, until the maximum bridge probability (among the unbuilt/available bridges) is above an arbitrarily small ϵ.

The Sequential Sampling Strategy, on the other hand, refers to the techniques that are used to estimate an unknown PDF by sampling from this unknown distribution and computing the histogram of these samples. The Metropolis-Hastings algorithm (MHA) is one of the most well-known sequential sampling algorithms [10]. The principal components of MHA are *i)* a sampling strategy, *ii)* a sample fitness function[3], $f(.)$ and *iii)* a candidate generating density, $q(.,.)$, which is the probability of generating a new sample from a given sample.

For a given seed tract S_i, the space whose PDF we wish to estimate, is composed of all fibers/clusters that S_i is part of. Let this set of clusters be denoted by $\Gamma_i^{(m)}$ where m is the sample index. With this setup, let us explain the principal ingredients of MHA as it is used in SMT :

[3] A sample fitness function is proportional to the probability of that sample, which is unknown.

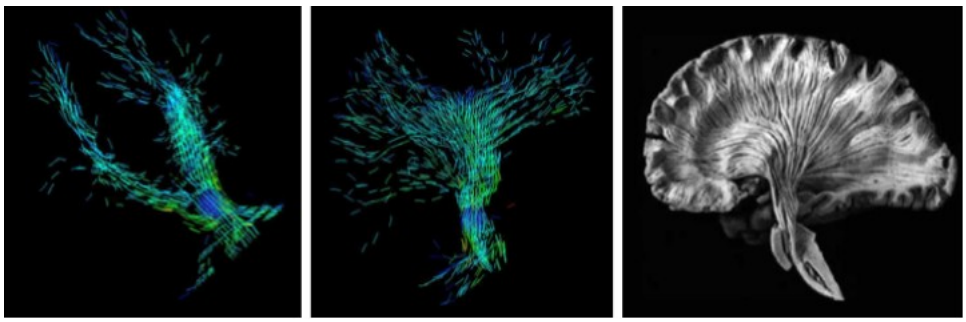

Fig. 3. SMT clusters corresponding to a ROI at the stem of the pyramidal tracts. The selected/displayed short tracts follow the normal anatomy closely as seen by comparison to the dissected brain image on the right

1. Sampling Strategy : Given a cluster of short tracts, $\Gamma_i^{(m)}$, the weakest bridge/link is broken. The strength of a link between $r_i^{(1)}$ and $r_j^{(k)}$ (see Equation 16) is measured by the *Fractional Anisotropy* of $D_i^{(1)}$, denoted by $F_i^{(1)}$. The rationale behind this is that bridges originating from nearly isotropic tensors are not reliable. The section of $\Gamma_i^{(m)}$ that includes S_i, the seed tract, is retained. A new bridge/link is built at random at the location of the broken one and the new cluster is formed by direct tracking as explained above.
2. Sample (Cluster/Fiber) Fitness : The fitness of a sample $\Gamma_i^{(m)}$, i.e. $f(\Gamma_i^{(m)})$ is chosen to be the minimum of the strengths of bridges/links that it includes. This is because a fiber's/cluster's reliability is dominated by the weakest link it includes.
3. Candidate Generating Density : Probability of generating a new sample candidate from a given sample is formulated as the product of the probability of breaking and building a bridge/link. It is given as,

$$q(\Gamma_i^{(m)}, \Gamma_i^{(m+1)}) = \underbrace{\frac{1/F_j^{(1)}}{\sum_{j\in A} 1/F_j^{(1)}}}_{\text{Prob. of Breaking a Link}} \times \underbrace{\frac{c_{j\to w}}{\sum_{w\in B} c_{j\to w}}}_{\text{Prob. of Building a Link}} \tag{17}$$

   where $F_j^{(1)}$ is the fitness of the broken bridge/link, $c_{j\to w}$ is the probability of the newly built link originating from $S_j^{(1)} \in \Gamma_i^{(m)}$, A is the set of short tract indices that belong to $\Gamma_i^{(m)}$ and B is the set of short tract indices that are in the neighbourhood of $r_j^{(1)}$, ie. the originating point of the broken bridge/link.

Following the MHA, the newly generated sample is accepted with a probability given as,

$$\alpha(\Gamma_i^{(m)}, \Gamma_i^{(m+1)}) = \min\left(1, \frac{f(\Gamma_i^{(m+1)}) q(\Gamma_i^{(m)}, \Gamma_i^{(m+1)}))}{f(\Gamma_i^{(m)}) q(\Gamma_i^{(m+1)}, \Gamma_i^{(m)})}\right) \tag{18}$$

If $\Gamma_i^{(m+1)}$ is accepted, then we increment $M_{in}, M_{ni} \quad \forall S_n \in \Gamma_i^{(m+1)}$, otherwise, we increment $M_{in}, M_{ni} \quad \forall S_n \in \Gamma_i^{(m)}$ by one. The whole process is repeated several times[4] Figure 3 shows SMT short tract clusters for an ROI on pyramidal tracts and the corresponding anatomy.

[4]The current implementation uses 100 samplings. However, as in all similar PDF estimation techniques, the more you sample, the better the approximation will be.

4. DISCUSSION

This manuscript attempts to highlight the inherent problems in DT-MRI analysis, esp. in fiber tractography. These inherent problems are due to the nature of the data itself. So, it is not possible to develop proper analysis, user interface and visualization tools without a thorough understanding of the data.

Widely accepted and useful DT-MRI analysis and visualization tools should consider that,

1. the DT-MRI data is based on signals averaged over subvolumes, ie. voxels,
2. the DT-MRI data assumes a Gaussian distribution of diffusing particles, whereas this assumption may be violated at fiber crossings,
3. the basic goal of these tools must be to present data loyally and communicate its information content as effectively as possible,
4. these tools should consider the spatial resolution of the data and should not pretend to have high resolution,
5. they should let the end-users draw the final and critical conclusions
6. the methods and the associated user-interfaces should allow for multiple seed point / ROI selection for the benefit formulazing a wider variety of analysis paradigms, such as, *Are these selected points connected ?*, *What is the path between the selected regions / points ?*, etc.

We have concentrated on two new analysis tools that attempt to fulfill these qualities. The other approach to the DT-MRI problem is to focus on visualization and user interface tools. We refer the reader to other manuscripts presented at SIMILAR NoE, WP10, Tensor Toolbox Workshop, for an introduction to state-of-the-art tools.

5. ACKNOWLEDGMENTS

This manuscript is based on the results of the research projects conducted with Erdem Yörük, Uğur Bozkaya, Roland Bammer, Chunlei Liu and Michael E. Moseley at Boğaziçi University, Istanbul, Turkey and Stanford University, Palo Alto, CA, USA. The research was supported in part by EU 6th Framework SIMILAR NoE and TUBITAK KARIYER-DRESS Project (104E035).

6. REFERENCES

[1] C. Liu, R. Bammer, B. Acar, and M.E. Moseley, "Characterizing non-gaussian diffusion by using generalized diffusion tensors," *Magnetic Resonance in Medicine*, vol. 51, pp. 924–937, May 2004.

[2] C.R. Tench, P.S. Morgan, M. Wilson, and L.D. Blumhardt, "White matter mapping using diffusion tensor mri," *Magnetic Resonance in Medicine*, vol. 47, pp. 967–972, 2002.

[3] M.A. Koch, D.G. Norris, and M. Hund-Georgiadis, "An investigation of functional and anatomical connectivity using magnetic resonance imaging," *Neuroimage*, vol. 16, pp. 241–250, 2002.

[4] P. Hagmann, J.P. Thiran, P. Vandergheynst, S. Clarke, and R. Meuli, "Statistical fiber tracking on dt-mri data as a potential tool for morphological brain studies," *ISMRM Workshop on Diffusion MRI : Biophysical Issues*, 2000.

[5] M.K. Chung, M. Lazar, A.L. Alexander, Y. Lu, and R. Davidson, "Probabilistic connectivity measure in diffusion tensor imaging via anisotropic kernel smoothing," Tech. Rep. 1081, University of Wisconsin, 2003.

[6] C. Lenglet, R. Deriche, and O. Faugeras, "Diffusion tensor magnetic resonance imaging : Brain connectivity mapping," Tech. Rep. 4983, INRIA, France, 2003.

[7] E. Yoruk, B. Acar, and R. Bammer, "A physical model for MR-DTI based connectivity map computation," MICCAI2005, Palm Springs, CA, USA, 2005, Lecture Notes in Computer Science, Vol. 3749 / Part 1, pp. 213–220.

[8] Ugur Bozkaya, "Smt : Split/merge fiber tractography for MR-DTI," M.S. thesis, Bogazici University, Bogazici University, Biomedical Engineering Institute, Istanbul, Turkey, 2006.

[9] U. Bozkaya and B. Acar, "Smt : Split/merge fiber tractography for MR-DTI," ESMRMB 2006, September 21-23 2006, Warsaw, Poland, 2006.

[10] S. Chib and E. Greenberg, "Understanding the metropolis-hastings algorithm," *The American Statistician*, vol. 49, pp. 327–335, 1995.